Int. J. Electrochem. Sci., 7 **(2012)** 8753 - 8760

International Journal of
ELECTROCHEMICAL
SCIENCE
www.electrochemsci.org

Preparation and Electrochemical Performance of $LiFePO_4$-based Electrode Using Three-Dimensional Porous Current Collector

Qiuming Wang, Dianlong Wang [*], *Bo Wang*

(School of Chemical Engineering and Technology, Harbin Institute of Technology, Heilongjiang 150001, PR China)
[*]E-mail: wangdianlonghit@163.com

Received: 19 July 2012 / *Accepted:* 13 August 2012 / *Published:* 1 September 2012

Three-dimensional (3D) porous current collector was introduced to improve the high-rate performance of the cells based on lithium iron phosphate ($LiFePO_4$). The 3D porous current collector was prepared by plating aluminium on the foam-type nickel substrate. The cells using the 3D porous current collector exhibited a superior high-rate performance as compared to the cells with conventional aluminum foil current collector. The results of EIS test indicated that the application of 3D porous current collector dramatically decreased the charge-transfer resistances for the positive electrode, owing to the large effective contact area between the active material particles and the current collector.

Keywords: Lithium iron phosphate ($LiFePO_4$); Three-dimensional porous current collector; High-rate performance

1. INTRODUCTION

Since demonstrated in 1997, orthorhombic lithium iron phosphate ($LiFePO_4$) [1], featuring a favorable theoretical capacity around 170 mAh/g, excellent cycling stability, low material cost, nontoxic and improved safety, has attracted considerable attention for the application in lithium ion battery which has been considered as one of the most promising power source for HEVs [2]. However, $LiFePO_4$-based batteries generally exhibit poor high-rate performance, since $LiFePO_4$ itself shows low conductivity. In order to improve the intrinsic drawback of $LiFePO_4$, many attempts have been performed, such as the doping with other cations and the coating with electronic conductive materials on the particles [3-5]. Besides, reducing the grain size is also an effective way to lessen the diffusion distance for lithium ion inside the electrode bulk [6-8]. Recently, a new method, modifying the structure of the electrode, has been introduced to improve the high-rate performance of the $LiFePO_4$-

based batteries [9-11]. In this paper, $LiFePO_4$-based electrodes using the three-dimensional (3D) porous current collector have been prepared and the influence of the 3D porous current collector on the high-rate and cycle-life performances has been examined.

2. EXPERIMENTAL

The 3D porous current collector was prepared by plating aluminium on the foam-type nickel substrate (400μm thick, 100PPI pore size, 500 g/m^2 surface density, Inco Co., China) from the THF type bath as similar as reported in literature [12]. The plating process was carried out inside an argon filled glove box, where the water and oxygen content was kept below 5 ppm. The electrolyte was obtained by evenly mixing $LiAlH_4$ solution (dissolved in THF) and $AlCl_3$ solution (dissolved in THF and benzene) with continuously stirring for 2 hours. The deposit was produced in current controlled (galvanostatic) conditions at room temperature, using double-anodes system of pure aluminium foils. All chemicals were obtained from Sinopharm Chemical Reagent Co.Ltd. The process parameters included bath composition, current density and plating time in this study, which were molar ratios of $AlCl_3/LiAlH_4$ (2:1, and $[AlCl_3] + [LiAlH_4]$ =1.3 mol/L), 0.5 A/dm^2 and 45 minutes, respectively.

The morphology and microstructure of foam-type nickel substrate and the as-prepared 3D porous substrate were characterized using field emission scanning electron microscopy (S4800, Hitachi). The electrochemical tolerance test using the cyclic voltammetric (CV) measurement was carried out on an electrochemical work station (CHI630A). The CV plots were recorded at a scan speed of 0.1 mVs^{-1}, with a potential range of 2.2–4.2V (*vs.* Li/Li^+, the foam-type nickel as the working electrode) and 3.0–4.8V (*vs.* Li/Li^+, the as-prepared 3D porous substrate as the working electrode), respectively. Lithium metal foils were used as the reference electrode and the counter electrode.

A well mixed slurry of the activated materials including $LiFePO_4$ (aleees, Taiwan), the electric conducting agent acetylene black (battery grade) and the binder PVDF (battery grade) in a ratio of 8:1:1 with NMP (battery grade) was plastered on the conventional aluminium foil substrate and the as-prepared 3D porous substrate respectively, and then dried at 120°C under vacuum for 6 hours to obtain the electrode. All electrodes were cut into disks with a diameter of 14 mm, and then stored in an argon-filled glove box.

For electrochemical measurements, 2025 button cells were assembled with the above disks as cathode, lithium metal foil as anode, a Celgard 2400 (polypropylene) as the separator, and EC/DMC/DEC-based (1:1:1 by weight) electrolytes containing 1M of $LiPF_6$. Charge-discharge rate capacity and cycle performance of the cells were tested on BTS Battery Testing system (Neware system, China), and the procedure was galvanostatic charge prior to constant voltage charge about 10 minutes, then galvanostatic discharge from 0.2*C* to 7*C* between 2.5V and 4V (*vs.* Li/Li^+). "*C*/n" means that the charge or discharge current is set up to achieve the nominal capacity (assuming $LiFePO_4$ as the active material) in "n" hours (e.g.3*C* corresponds to a charge or discharge in 20 min, and the current is ca. 510 $mA \cdot g^{-1}$). Electrochemical impedance measurements of the cells were carried out with an electrochemical workstation (PARSTAT 2273, U.S.A.) at room temperature. The frequency range was from 100 kHz to 0.01 Hz with an AC signal amplitude of 5mV.

3. RESULTS AND DISCUSSION

Fig 1 shows the SEM images of the foam-type nickel substrate, the as-prepared 3D porous substrate and $LiFePO_4$-based electrode using the 3D porous substrate as current collector. The thickness of aluminum coating on the foam-type nickel substrate is about 10μm (c). The 3D porous current collector has a large surface area due to its unique framework structure, which improves the current collecting ability as well as increases the loading amounts of the active materials effectively.

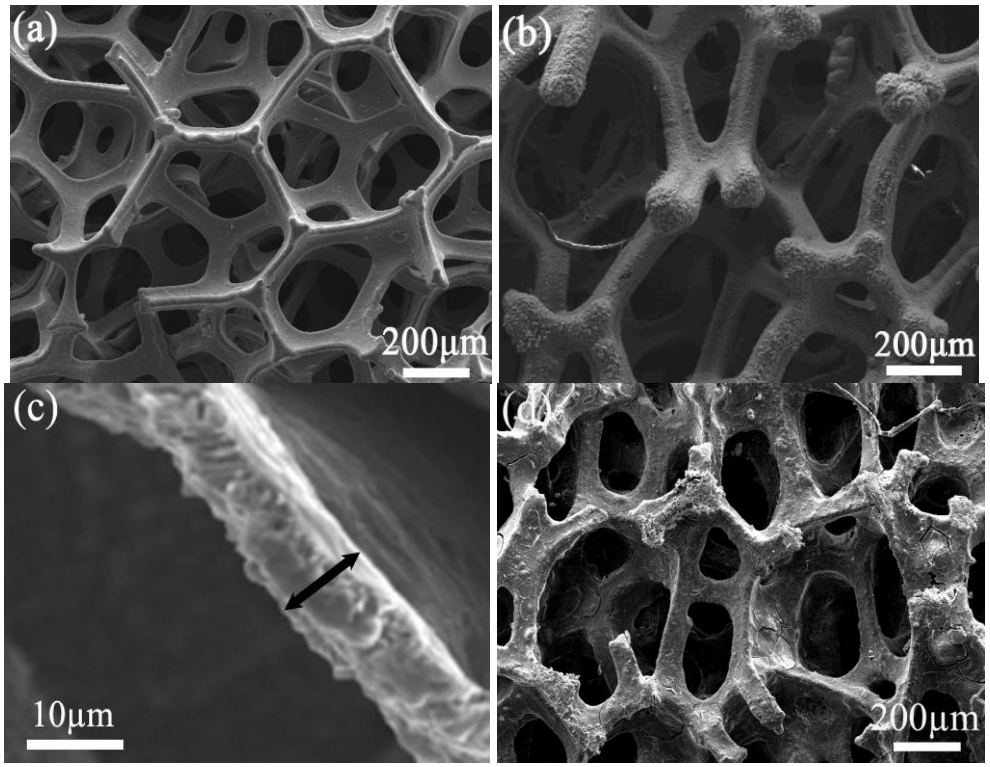

Figure 1. SEM images of the foam-type nickel (a), the as-prepared 3D porous substrate (b), cross-section view of aluminum coating on the foam-type nickel substrate (c) and $LiFePO_4$-based electrode using the as-prepared 3D porous current collector (d)

Fig.2 shows the CV plots which were recorded during the electrochemical tolerance test. A high anodic potential can be observed for the as-prepared 3D porous substrate (b) compared with the foam-type nickel substrate (a). The foam-type nickel exhibits a growing current curve above around 3.5V owing to corrosion. Just for this reason, foam-type nickel substrate is usually used in anode rather than in cathode for lithium ion battery [13-15]. In contrast, the 3D porous substrate exhibits a much smaller anodic current at about 4.4V. This polarization behaviour is attributed to the formation of a passivation film on the surface of aluminium, which improves the electrochemical tolerance of the substrate. Fig.3 shows the charge-discharge voltage curves of the cells using the 3D porous current collector and the aluminium foil current collector. The loading amounts of the active materials are around $130g/m^2$ and $50g/m^2$, respectively. Both the cells exhibit almost the same performance at 0.2*C* and 1*C*, with a specific capacity around 150 $mAh \cdot g^{-1}$ and 130 $mAh \cdot g^{-1}$ respectively. However, the specific capacity of the cell using the aluminium foil current collector is only around 90 $mAh \cdot g^{-1}$ at

5*C*, which is 20 mAh·g^{-1} less than that of the cell using the 3D porous current collector. The gap of the specific capacity widens up at 7*C*, which is about 35 mAh·g^{-1}.

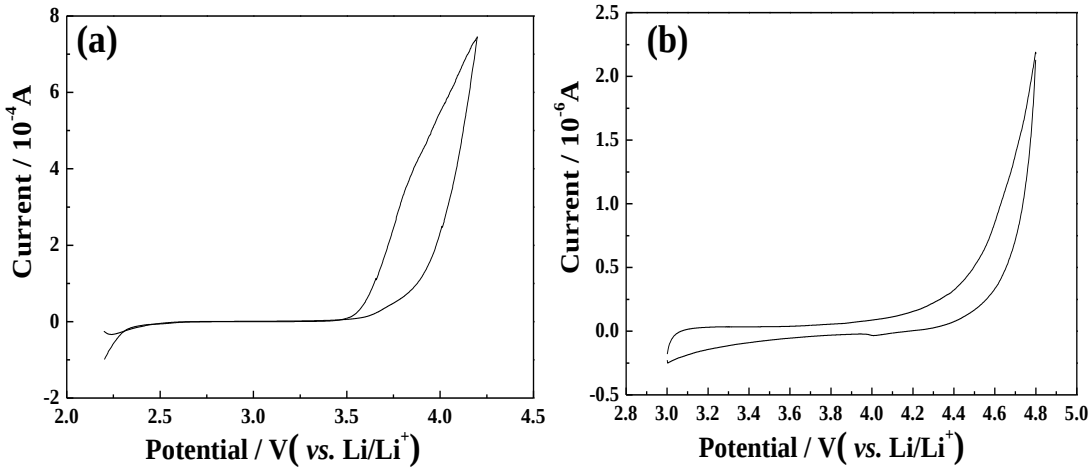

Figure 2. CV plots of the foam-type nickel (a) and the as-prepared 3D porous substrate (b) recorded during the electrochemical tolerance test

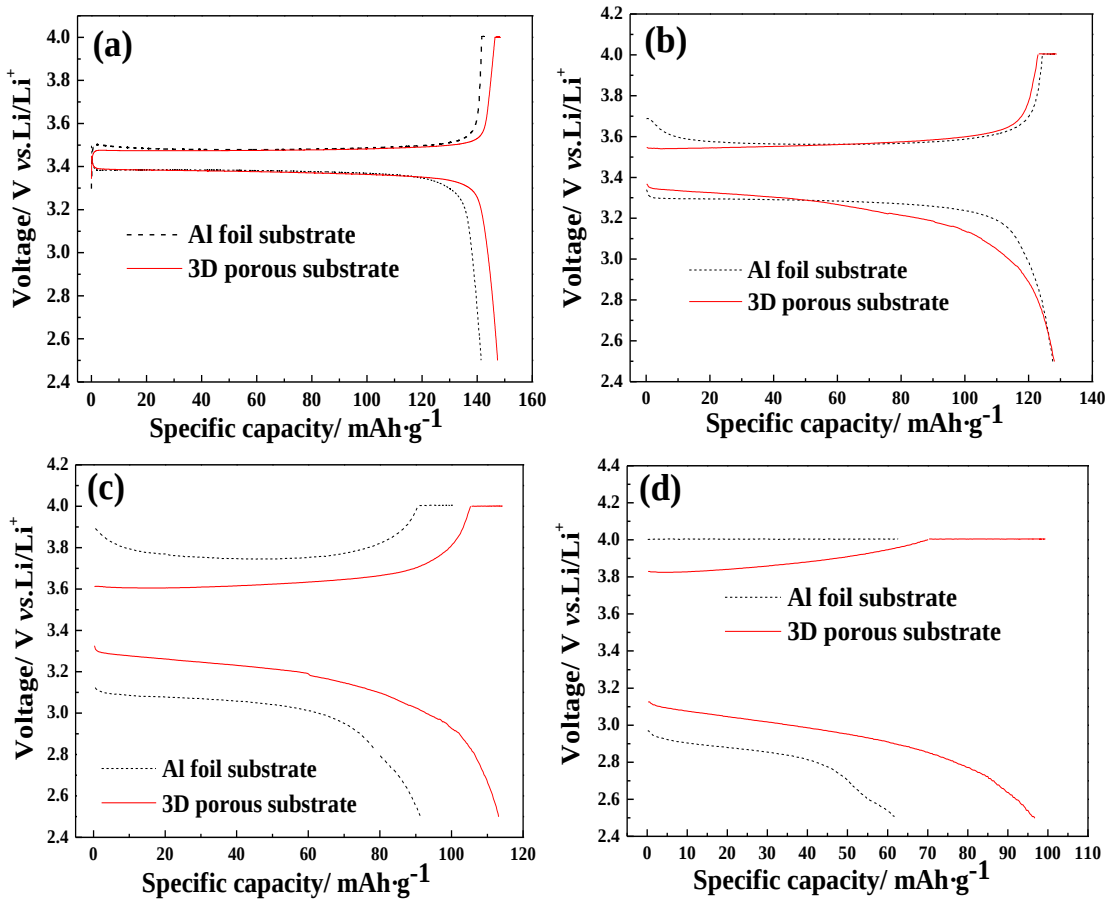

Figure 3. Charge-discharge voltage curves of $LiFePO_4$-based cells using the 3D porous current collector and the aluminium foil current collector at different rates (a) 0.2*C* (b) 1*C* (c) 5*C* (d) 7*C*

Besides, the polarization between the charge and discharge plateaus of the cell using the 3D porous current collector is also less than the one with aluminium foil current collector, especially at high rates. The results indicate the superiority of 3D porous current collector in charge-discharge test at high rates.

Fig.4 shows the cycle-life profiles of the cell using the 3D porous current collector. The capacity loss of the cell is less than 5% at each rate after 20 cycles, which is comparable as the cell using the aluminium foil current collector. The deficiency in cycle stability of $LiFePO_4$-based electrode with the foam-type nickel current collector has been demonstrated by Yao [16], which is also in accordance with the results of our preparatory experiment. The improvement of the cycle performance implies the improved corrosion resistance property of the current collector, owing to the existence of aluminium coating on the foam-type nickel substrate.

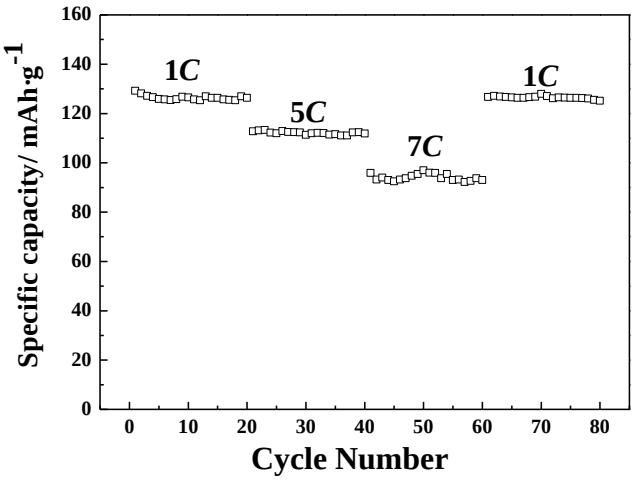

Figure 4. Cycle-life profiles of $LiFePO_4$-based cell using the 3D porous current collector

Electrochemical impedance spectroscopy (EIS) is introduced to investigate the cells in detail after cycle-life test. The Nyquist plots of the cells using different current collectors as well as the fitted curves of EIS data are shown in Fig.5. Each plot is composed of a depressed semicircle from the high-frequency region to mid-frequency region and a sloping line in the low-frequency region.

To perform a quantitative analysis, an equivalent circuit, as shown in Fig.6, is proposed to fit the impedance spectra and the fitting results are listed in Table 1. R_0 refers to the ohmic resistance of the two-electrode cell, including the resistance of the electrolyte, electrode leads and terminals. Warburg impedance W represents the diffusive behavior. A resistance R_A in parallel with an ideal capacitor C_A is assigned to the lithium migration through several SEI layers in anode [17, 18]. There are two RQ-elements，$Q_{C1}R_{C1}$ and $Q_{C2}R_{C2}$, representing the polarization processes in cathode. Based on the earlier research, $Q_{C1}R_{C1}$ is used to signify the interface between cathode composite and aluminum foil current collector [17, 19, 20] and $Q_{C2}R_{C2}$ shows the charge-transfer process between electrolyte and cathode composite [20, 21].

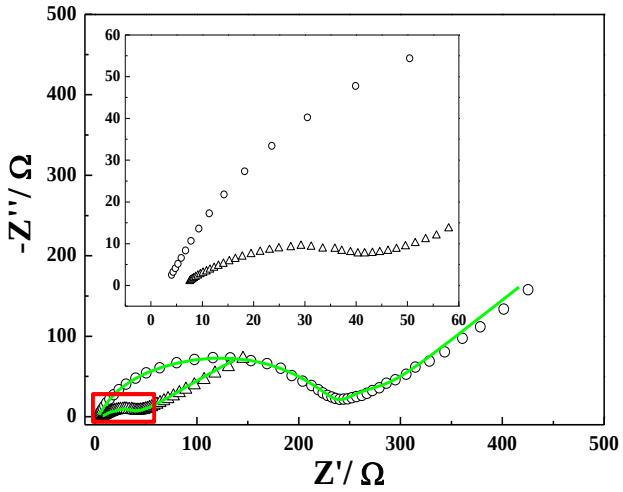

Figure 5. Nyquist plots of $LiFePO_4$-based cells using the 3D porous current collector (△) and the aluminium foil current collector (○)

The *RQ*-elements as well as C_AR_A process consist of the depressed semicircle in each Nyquist plot, in which the electrochemical processes are difficult to be distinguished, owing to the overlap of the polarization process [17, 21].

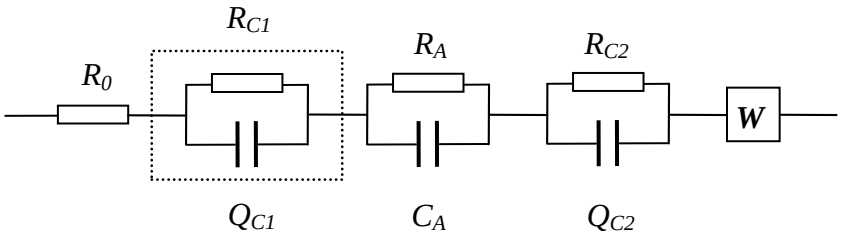

Figure 6. Equivalent circuit model of $LiFePO_4$-based cells using different current collectors

However, as to the cell using the 3D porous current collector, there is no $Q_{C1}R_{C1}$ process in the equivalent circuit. The result implies this process only causes a minor part of the overall cell impedance, which can be neglected in the equivalent circuit [17]. Besides, the fitting result of R_{C2} is much smaller than that of the cell using the aluminium foil current collector. The disappearance of $Q_{C1}R_{C1}$ process and the reduction of R_{C2}, corresponding to the obvious difference in the size of the depressed semicircles, indicate the charge-transfer resistances for the positive electrode dramatically decreases due to the application of 3D porous current collector which provides a large effective contact area between the active material particles and the current collector. The variation of the charge-transfer resistances can be used to interpret the result shown in Fig.3. At a low rate, the effect of a large charge-transfer resistance can be neglected, but for higher rates the charge-transfer resistance is mainly responsible for the voltage rise (charge) or drop (discharge) causing a sudden decrease in the electrochemical performance.

Table 1. Equivalent circuit parameters obtained from fitting the impedance Spectra in Fig.6

Parameters	The cell with the 3D porous current collector	The cell with the Al foil current collector
R_0/Ω	4.425	2.935
R_{C1}/Ω	—	22.26
Q_{C1}-n	—	0.9412
Q_{C1}-$Y_0/\Omega^{-1}\cdot s^n$	—	1.131 E-5
R_A/Ω	17.94	18.62
C_A/F	0.059	0.01435
R_{C2}/Ω	44.46	211.4
Q_{C2}-n	0.5636	0.727
Q_{C2}-$Y_0/\Omega^{-1}\cdot s^n$	0.001127	2.699 E-5
W-$Y_0/\Omega^{-1}\cdot s^{0.5}$	0.0399	0.01752

4. CONCLUSION

Three-dimensional porous current collector, which displayed higher tolerance in organic electrolytes as compared to the foam-type nickel, was prepared for $LiFePO_4$-based cells by plating aluminium on the foam-type nickel substrate. The SEM images indicated the 3D porous current had a large surface area due to the unique framework structure. The $LiFePO_4$-based cells using the 3D porous current collector exhibited a superior high-rate performance, compared to the cells with the conventional aluminum foil current collector. In the electrochemical impedance measurements, the application of 3D porous current collector dramatically decreased the charge-transfer resistances for the positive electrode, which can be ascribed to the large effective contact area between the active material particles and the current collector. The application of the 3D porous current collector in $LiFePO_4$-based cells indicates that it is feasible to improve the high-rate capability of the high-power lithium ion batteries by designing and modifying the structure of electrode.

ACKNOWLEDGMENTS

This work has been supported in part by National Natural Science Foundation of China (No. 50974045), the Ph. D Programs Foundation of Ministry of Education of China (No. 20092302110052) and the Natural Science Foundation of Heilongjiang Province, China (No. B200918)

References

1. A.K. Padhi, K.S. Nanjundaswamy, J.B. Goodenough, *J. Electrochem. Soc.*, 144 (1997) 1188.
2. A. Chu, P. Braatz, *J. Power Sources*, 112 (2002) 236.
3. Y.S. Hu, Y.G. Guo, R. Dominko, M. Gaberscek, J. Jamnik, *Adv. Mater.*, 19 (2007) 1963.
4. B. Jin, E.M. Jin, K.-H. Park, H.-B. Gu, *Electrochem. Commun.*, 10 (2008) 1537.
5. D.-W. Han, Y.-M. Kang, R.-Z. Yin, M.-S. Song, H.-S. Kwon, *Electrochem. Commun.*, 11 (2009) 137.

6. F.Yu, J.J. Zhang, Y.F. Yang, G.Z. Song, *J. Mater. Chem.*, 19 (2009) 9121.
7. X.L. Wu, L.Y. Jiang, F.F. Gao, Y.G. Guo, L.J. Wan, *Adv. Mater.*, 21 (2009) 2710.
8. C. Sun, S. Rajasekhara, J.B. Goodenough, F. Zhou, *J. Am. Chem. Soc.*, 133 (2011) 2132.
9. M. Yao, K. Okuno, T. Iwaki, T. Awazu, T. Sakai, *J. Power Sources*, 195 (2010) 2077.
10. M.M. Shaijumon, E. Perre, B. Daffos, P.-L. Taberna, J.-M. Tarascon, P. Simon, *Adv. Mater.*, 21 (2010) 4978.
11. M. Roberts, P. Johns, J. Owen, D. Brandell, K. Edstrom, G.E. Enany, C. Guery, D. Golodnitsky, M. Lacey, C. Lecoeur, H. Mazor, E. Peled, E. Perre, M.M. Shaijumon, P. Simon, P.-L Taberna, *J. Mater. Chem.*, 21 (2011) 9876.
12. Q. Chen, D. Tan, R. Liu, W. Li, *Surf. Coat. Technol.*, 205 (2011) 4418.
13. Q. Sa, Y. Wang, *J. Power Sources*, 208 (2012) 46.
14. C. Wang, D. Wang, Q. Wang, L. Wang, *Electrochim. Acta*, 55 (2010) 6420.
15. C. Yang, D. Zhang, Y. Zhao, Y. Lu, L. Wang, J.B. Goodenough, *J. Power Sources*, 196 (2011) 10673.
16. M. Yao, K. Okuno, T. Iwaki, M. Kato, S. Tanase, K. Emurab, T. Sakai, *J. Power Sources*, 173 (2007) 545.
17. J. P. Schmidt, T. Chrobak, M. Ender, J. Illig, D. Klotz, E. Ivers-Tiffée, *J. Power Sources*, 196 (2011) 5342.
18. A. Zaban, E. Zinigrad, D. Aurbach, *J. Phys. Chem.*, 100 (8) (1996) 3089.
19. M. Gaberscek, J. Moskon, B. Erjavec, R. Dominko, J. Jamnik, Electrochem. *Solid-State Lett.*, 11 (10) (2008) A170.
20. N. Schweikert, H. Hahn, S. Indris, *Phys. Chem. Chem. Phys.*, 13 (2011) 6234.
21. D. Zane, M. Carewska, S. Scaccia, F. Cardellini, P. P. Prosini, *Electrochim. Acta*, 49 (2004) 4259.